

Published in: *J. Electrochem. Soc.* 163 (9), pp. D485-D492, 2016

Influence of Pb additive to the spacer layer on the structure and giant magnetoresistance of electrodeposited Co/Cu multilayers

M. Jafari Fesharaki^{a,b}, K. Neuróhr^a, L. Péter^a, Á. Révész^c,

L. Pogány^a, G. Molnár^d, I. Bakonyi^{a,*}

^a*Wigner Research Centre for Physics, Hungarian Academy of Sciences.
H-1121 Budapest, Konkoly-Thege út 29-33, Hungary*

^b*Department of Physics, Payame Noor University, P.O.Box 19395-3697, Tehran, Iran*

^c*Department of Materials Physics, Eötvös University.
H-1117 Budapest, Pázmány Péter sétány 1/A, Hungary*

^d*Institute for Materials Science and Technical Physics, Energy Research Centre,
Hungarian Academy of Sciences. H-1121 Budapest, Konkoly-Thege út 29-33, Hungary*

ABSTRACT – In an effort to see the possible surfactant effect of Pb on the formation of electrodeposited multilayers, Co/Cu(Pb) multilayers were prepared by this technique and their structure and giant magnetoresistance (GMR) were investigated. The multilayers were deposited from a perchlorate bath with various amounts of Pb²⁺ ions in the solution. The composition analysis by energy dispersive X-ray spectroscopy revealed that the Pb mole fraction in the deposit varies in a non-monotonous manner with Pb²⁺ ion concentration. By fitting the measured X-ray diffraction patterns, superlattice satellites could be identified in some of these multilayers. A ferromagnetic-type GMR behavior was observed for Co/Cu(Pb) deposits prepared from baths with small Pb²⁺ ion concentration, corresponding to the formation of a layered structure. The GMR magnitude decreased from 8 to 10 % with increasing Pb concentration and, also, changed to a superparamagnetic-type GMR; finally, for high Pb²⁺ ion concentrations, the magnetoresistance behavior turned over to anisotropic magnetoresistance characteristic of bulk materials.

KEYWORDS: electrodeposition, Co/Cu multilayer, Pb additive, GMR

*Corresponding author. E-mail: bakonyi.imre@wigner.mta.hu

Introduction

The application of so-called surfactant elements in multilayer growth has become a common practice for physical deposition methods. The importance of the use of surfactant elements such as, e.g., Pb, Ag, Bi, Au and In is that their presence on the substrate during layer formation can efficiently promote layer-by-layer growth since they can alter the kinetics of the deposition of adatoms and their incorporation into the existing metal lattice, as well as the surface energy of the growing deposit [1-3]. The use of Pb as surfactant was found to have a particularly profound effect on the layer quality of Co/Cu multilayers [2,4,5], leading to a virtually nucleation-free growth and even layer thicknesses. The improved layer quality concomitantly resulted in better physical properties such as stronger antiferromagnetic coupling and higher giant magnetoresistance (GMR) [5-10].

In an effort to improve the still inferior GMR characteristics of electrodeposited multilayers [11] with respect to their physically deposited counterparts, it was decided to study the influence of some surfactants on the formation and GMR of electrodeposited Co/Cu multilayers. Unfortunately, due to solubility and electrochemical compatibility limitations, the codeposition of the common surfactant elements with Co and Cu from a single bath is not a straightforward task. The codeposition of Co, Cu and Ag could be successfully carried out [12] from a perchlorate type solution into which all the metal anions were introduced by using their perchlorate salts with ClO_4^- anions on the basis of earlier reported experiences [13,14]. This type of bath proved to be able to yield Co/Cu(Ag) multilayer deposits on which both structural and magnetoresistance studies could be performed [12]. It was found that a small amount of Ag (until about 1 at.% of Ag in Cu) incorporated in the spacer layer induced, indeed, an improvement of the GMR magnitude. However, for larger Ag contents in the samples, a strong structural degradation occurred which was accompanied by a significant reduction of the GMR magnitude.

We have also tried to explore the influence of Bi as a surfactant on the GMR of electrodeposited Co/Cu multilayers [15]. Since the solubility of most of the Bi salts is very low in moderately acidic solution, the acetate, sulfate and sulfamate type solutions for preparing Co/Cu multilayers were compared to those saturated with Bi_2O_3 . Due to the very low Bi^{3+} ion concentration achieved in these solutions, practically no influence of the Bi^{3+} ion addition on the GMR could be demonstrated [15]. Upon a large pH change, the multilayer quality deteriorated even without the addition of the bismuth compound, in accord with some previous observations [11,16]. As far as the chloride-based bath is concerned, BiCl_3 could be

employed as a bismuth source, but a very low pH had to be provided to achieve an appreciable solubility. Besides the fact that chloride anions in a sulfate-based bath have a negative influence on the GMR of electrodeposited Co/Cu multilayers [17], the experimental conditions altogether led to bad deposit quality without a multilayer structure and resistivity measurements were not possible.

As a next step, we intended to carry out a similar study in order to explore the influence of Pb when added as surfactant to the Cu spacer layer of electrodeposited Co/Cu multilayers. In a recent work [18], we have investigated the codeposition of Co and Pb from acetate-, chloride- and nitrate-based baths out of which the acetate bath only yielded compact Co-Pb deposits. Although compact Co/Cu(Pb) multilayers could be successfully prepared from such a bath, the magnetoresistance measurements performed on these samples have not provided reliably reproducible results. On the other hand, based on the experiences with a perchlorate-based bath for electrodepositing Co/Cu(Ag) multilayers [12], we could successfully produce electrodeposited Co/Cu(Pb) multilayers from this type of bath which were appropriate for studying their GMR characteristics.

Along this line, the present paper describes the results of our experiments on electrodeposited Co/Cu(Pb) multilayers from a perchlorate bath in order to reveal the influence of Pb incorporated in the spacer layer on the GMR of these multilayers. In addition, X-ray diffraction (XRD) measurements have also been performed in order to establish the structural evolution of these multilayers in the presence of Pb surfactant.

Experimental

Materials and chemicals. — The Co/Cu(Pb) multilayers for the present study were electrodeposited from perchlorate-based solutions. All chemicals used for the solution preparation were of analytical grade from Alfa Aesar except where otherwise noted. The bath compositions were optimized under the condition to yield continuous and fairly smooth compact deposits which can be reliably contacted for magnetoresistance measurements. Two stock solutions were used in the experiments.

The first stock solution contained $\text{Co}(\text{ClO}_4)_2$ (0.2 or 0.4 mol dm⁻³), $\text{Cu}(\text{ClO}_4)_2$ (0.015 mol dm⁻³) and H_3BO_3 (0.2 mol dm⁻³; Reanal) and the pH was 4.55. The second one contained $\text{Pb}(\text{ClO}_4)_2$ instead of $\text{Cu}(\text{ClO}_4)_2$ but with the same metal ion concentration, while the other components and their concentrations were the same as in the first electrolyte. The two

different $\text{Co}(\text{ClO}_4)_2$ concentrations were chosen in order to reveal a possible influence of the magnetic metal ion concentration on the nucleation process during multilayer formation.

Finally, an appropriate mixture of the two perchlorate stock solutions was used for the preparation of electrodeposited Co/Cu(Pb) multilayers with various Pb concentrations in the spacer layer. The Pb^{2+} ion concentration of the electrolyte solution used for multilayer preparation will be given with the following ratio throughout the entire work: $[\text{Pb}^{2+}]/([\text{Pb}^{2+}] + [\text{Cu}^{2+}])$.

Cyclic voltammetry characterization of the electrolytes. — Cyclic voltammograms (CV) were recorded for electrolytes with various Pb^{2+} ion concentrations at a scan rate of 5 mV/s in order to reveal the potential ranges of the deposition of the three components (Co, Cu and Pb). The substrate was a Pt sheet in these experiments with an exposed surface area of 0.608 cm^2 . The solution was stagnant, similarly to the conditions applied for the sample preparation procedure.

Sample preparation. — Electrodeposition was performed at ambient conditions in a tubular cell with an upward facing horizontal cathode of about 1.5 cm^2 surface area [19,20]. An EF453 type potentiostat/galvanostat (Electroflex, Hungary) served as current source. A saturated calomel electrode (SCE) was used as reference which was connected to the cell via an external vessel filled up with an electrolyte solution without Pb^{2+} but otherwise identical to the bath used for deposition.

The substrate was a metal-coated Si wafer with the (100) orientation. A 5-nm-thick Cr adhesive layer was followed by a 20-nm-thick Cu conductive layer; both layers were produced by evaporation. The mean surface roughness of the Si/Cr/Cu substrates determined with atomic force microscopy was found to be between 1 and 3 nm [21]. A Cu sheet served as counterelectrode in each case.

A galvanostatic/potentiostatic (G/P) pulse combination [11,19,22] was used to produce the Co/Cu(Pb) multilayers. The magnetic Co layer was deposited in galvanostatic mode at -19.2 mAcm^{-2} current density. For establishing the optimum potential for the deposition of the non-magnetic layer, an analysis of the current transients following the magnetic layer deposition pulse was applied [11,22]. For the Co-Cu-Ag perchlorate bath, this optimum potential was established as -585 mV vs. SCE for each Ag^+ ion concentration investigated in our previous work [12] and this value was applied for the deposition of the non-magnetic

layers also in all Co/Cu(Pb) multilayers here. The use of an optimized non-magnetic layer deposition potential ensures that neither dissolution of the previously deposited magnetic layer (Co) nor codeposition of the magnetic atoms into the non-magnetic layer can occur, the consequence of which is that the actual layer thicknesses will be equal to the nominal values preset on the basis of Faraday's law.

The nominal thicknesses of the magnetic and non-magnetic layer were fixed at 3 nm and 7 nm as was the case for the electrodeposited Co/Cu(Ag) multilayers [12]. The number of bilayer repetitions was chosen to give a total multilayer thickness of about 800 nm. For each electrolyte, 100 % current efficiency was assumed for both kinds of layer.

Composition analysis — The overall composition of the multilayer films was determined by energy-dispersive X-ray spectroscopy (EDX) in a JEOL JSM 840 scanning electron microscope. The RÖNTEC EDX unit equipped with a Si detector was operated at 25 kV. The chemical analysis was carried out for spots of about 1 mm² surface area each. The composition was measured on at least three different spots for every sample.

Structural study — The structure of the Co/Cu(Pb) multilayers was investigated by recording wide-angle XRD patterns with Cu-K_α radiation on a Philips X'pert powder diffractometer in Θ -2 Θ geometry. The step width was 0.02 degree in the range of 20-100 degree.

Magnetoresistance measurements — The magnetoresistance (MR) characteristics of the deposits were studied at room temperature. The magnetoresistance was measured with a 4-point-in-line probe up to $H = 8$ kOe external magnetic field in the field-in-plane, current-in-plane configuration. The magnetoresistance was measured for both the longitudinal (LMR) and transverse (TMR) components with the magnetic field and the current parallel and perpendicular to each other, respectively. The MR ratio was defined as $\Delta R/R_0 = [R(H) - R_0]/R_0$ where $R(H)$ and R_0 are the resistance values measured in a magnetic field H and at the resistance peak around zero magnetic field, respectively.

Results

Cyclic voltammograms. — The CV curves are shown in Figs. 1 and 2 for the perchlorate electrolytes containing 0.2 and 0.4 mol dm⁻³ Co(ClO₄)₂ concentrations, respectively, with varying Pb²⁺ concentration. Although a large number of cyclic voltammograms were recorded for all solutions used, Figs. 1 and 2 display the curves recorded with -875 mV negative potential limit only for the sake of highlighting the Cu (and Pb) deposition regime and the difference in the nucleation behavior of Co under various circumstances. For each Pb²⁺ ion concentration, the displayed CV curve corresponds to the first scan on a fresh Pt surface and a homogeneous solution.

The Cu deposition started between +30 mV and +2 mV vs. SCE in all experiment. The variation of the Cu deposition onset potential could not be unambiguously correlated to the Pb²⁺ content of the solution. The voltammograms showed one single wave (often with a small peak) after the start of the Cu deposition. The limiting current density of the Cu (and perhaps Pb) deposition was between -1.00 and -1.12 mAcm⁻², regardless of the lead-to-copper ratio of the solutions used. At the Pb²⁺ concentrations applied, the deposition of Cu and Pb could not be separated in the voltammograms. In a non-complexing bath with similar Co²⁺ concentration (which can be regarded as a supporting electrolyte at potentials more positive than the Co nucleation), the onset of the Pb deposition was found to be at -545 mV vs SCE [18]. Around this potential, there was no sign of the occurrence of a new phase in the voltammograms shown in Figs. 1 and 2. Since Pb and Cu are immiscible, the deposition of Pb should manifest itself by a new nucleation step and with some nucleation overpotential as compared to the equilibrium potential of the Pb²⁺/Pb system. Although Pb can form a monatomic underpotential layer on the (111) Cu surface at more positive potentials than the bulk Pb deposition [23-26], this could not be identified in either of the voltammograms recorded.

Although the current density in the potential regime of diffusion-limited Cu deposition did not seem to be sensitive to the Pb²⁺ concentration applied, the onset potential of the Co codeposition showed a very unusual dependence on the Pb²⁺ concentration. The larger was the Pb²⁺ ratio in the solution, the less negative was the Co nucleation potential. At 5 % Pb²⁺ content of the solution, the current increase due to the Co nucleation started at 80 mV more positive potential than in the absence of Pb²⁺. Apparently, the presence of Pb, as a component of either of the newly forming substrate or the solution, has a promoting impact on the Co nucleation. This is surprising if one takes into account that Pb is not miscible with Co and,

therefore, the shift in the nucleation potential cannot be explained by the formation of a new alloy phase. The current related to the Co deposition at the negative limit of the voltammograms shown is more than 2.5 times larger than without Pb^{2+} in the solution.

After the change in the sweep direction, the cathodic current measured remains larger than at the same potential in the negative-going scan. This behavior is typical if the deposition of the metal studied can nucleate on the substrate with large activation energy only. In such cases, the deposition after the scan reversal takes place already on the parent metal. The Co deposition in parallel to the Cu deposition can be maintained as long as the Cu being deposited does not fully cover the cathode. As it can be seen in the voltammograms in Figs. 1 and 2, the presence of Pb significantly suppresses the ability of Cu to completely cover the cathode, and when the Pb^{2+} concentration is as high as 5%, the Co nuclei can grow until the equilibrium potential of the Co^{2+}/Co pair is reached. This is clearly indicated by the absence of the flat region in the anodic-going curves at high Pb content, and the current density returns to the diffusion-limited Cu deposition current density only immediately prior to the onset of Co dissolution. The position of the inflection point of the voltammograms at high Pb concentration indirectly verifies the optimized Cu deposition potential applied that corresponds to the equilibrium potential of the Co^{2+}/Co redox pair.

The increase in the cathodic current at the most negative potentials applied in the cathodic-going scans and the upcoming large cathodic current on the negative part of the anodic-going scan are accompanied by the development of a peak in the anodic scan, corresponding to the dissolution of the Co deposited. The charge corresponding to the Co dissolution monotonously increases with the Pb content of the solution. Although the Co stripping peak splits up into two humps, especially in the curves recorded from the 0.4 M $\text{Co}(\text{ClO}_4)_2$ solution, this phenomenon cannot be ascribed to the development of a Pb dissolution peak since Co tends to exhibit such double peak in various media [14,22,27-30], irrespectively of any other metallic components present.

After the dissolution of Co available from the solution (i.e., not covered subsequently by Cu), the current returns to a negative value, corresponding to Cu deposition at potentials less than about +30 mV. The rising arms of the Cu dissolution peaks in the subsequent sweeps fully coincide, while the end of the stripping peak depends on the overall amount of Cu deposited.

Although the Cu dissolution peak for both Co^{2+} concentrations represents the least charge at 5% Pb^{2+} content, the impact of the lead ions to the Cu deposition is rather controversial. The charge passed during the sweeps shown in Figs 1 and 2 from the start of the measurement

until the onset of Cu dissolution is 0.372 C cm^{-2} for 0 and 1% solutions, and the dissolution of Cu corresponds to 0.354 C cm^{-2} on the average. The small difference (about 5%) is ascribed to the deviation of the current efficiency from 1, especially at high negative potentials where Co can also be deposited. However, at 5% Pb^{2+} content this difference is much higher. While the charge measured until the onset of Cu dissolution was 0.511 C cm^{-2} , the Cu dissolution corresponds to 0.282 C cm^{-2} only. The difference is very large and cannot be attributed to a loss in the current efficiency. This view is further supported by the figures that refer to the Co deposition and dissolution only. If the charge corresponding to Co deposition and dissolution is compared by correcting the current densities with the contribution of Cu deposition, the difference is less than 2% for all baths. Therefore, the change in the current efficiency does not play a significant role in the occurrence of the charge imbalance.

It is rather thought that morphological parameters are of high importance here. Qualitative deposit tests indicated that the porosity of Cu deposits increases with both the deposition potential and the Pb content of the bath (this observation is based on the optical microscopic observation of the deposits). Hence, if the dissolution is not exactly the reversal of the deposition process, the dissolution of the deposit with high surface area may lead to the disintegration of solid particles, which is observed as a loss in charge. Morphological effects may also play some role in the formation of the shape of the peaks in the voltammograms. Since Pb does not form an alloy with either of the other elements present, the disturbance of the layer formation of Cu on Co may explain the much compressed flat region of the anodic-going scans prior to the Co dissolution. Without any other factor, the structure-breaking impact of the codeposited Pb can explain all observations.

Although the conditions of the experiments related to the cyclic voltammetry measurements and the multilayer sample preparation are different, it is worthwhile of noting that the CV curves do not indicate the formation of a significant amount of chloride ions from the perchlorate anions. In the presence of an appreciable amount of chloride ions, the Cu deposition wave should split up into two current steps of equal height because of the stabilization of the $[\text{CuCl}_2]^-$ species. For the same reason, the dissolution of Cu in the presence of chloride ions should take place as Cu(I) instead of Cu(II).

The instability of the perchlorate ions in the potential regime of the deposition of transition metals is straightforward from the relevant Pourbaix diagram [31]. It is also known that in the presence of corroding transition metals perchlorate ions may decompose [32]. Data on the kinetics of the perchlorate decomposition on corroding cobalt in acidic media are also

available [33,34]. Nevertheless, we have not observed any sign of bath instability due to the reduction of perchlorate anions.

Overall chemical composition analysis. — The impact of Pb^{2+} ion concentration in the perchlorate bath on deposit composition was studied by a gradual replacement of Cu^{2+} ions with Pb^{2+} ions in the electrolyte. The concentrations of the constituent metals in the multilayered deposits are displayed in Fig. 3 as a function of the ionic ratio $[\text{Pb}^{2+}]/([\text{Pb}^{2+}] + [\text{Cu}^{2+}])$ in the bath. At low Pb^{2+} ion concentrations, the Co and Cu contents exhibit a strongly non-monotonous variation and are completely in antiphase to each other. Above 2 at. % Pb^{2+} ion concentration, the Co and Cu concentrations remain roughly constant. The Pb content in the multilayered deposits remains much smaller for the whole Pb^{2+} ion concentration range studied. As it can be seen in the magnified view of the Pb mole fraction data, the deposit Pb content first increases with the Pb^{2+} ion concentration of the electrolyte, then decreases, exhibiting a maximum around 1.5 % Pb^{2+} ratio in the solution. This indicates that the codeposition of Co, Cu and Pb takes place according to a complicated process and the mechanism causing the unusual codeposition behavior of Pb is still unknown.

Structural study by XRD. — The XRD patterns were recorded for some of the multilayers with various Pb^{2+} ion concentrations and with either 0.2 or 0.4 M $\text{Co}(\text{ClO}_4)_2$ concentration in the perchlorate bath. All observed XRD patterns could be indexed to a face-centered cubic (fcc) structure, with the Bragg peak positions in between the corresponding positions for pure fcc-Cu and fcc-Co as was found also for the electrodeposited Co/Cu(Ag) multilayers [12]. A very strong (111) texture was observed in each case: the intensity of the (111) peak was typically 5 to 10 times higher than the intensity of the (200) peak, with the difference being somewhat smaller for higher Pb^{2+} ion concentrations in the bath.

The XRD peaks near the main (111) fcc-Co/Cu multilayer reflection are shown in Fig. 4a for three samples prepared without Pb^{2+} ion addition to the perchlorate bath. For the multilayer prepared with 0.4 M $\text{Co}(\text{ClO}_4)_2$ concentration in the bath, the shoulders marked by the arrows on both sides of the main (111) peak can be assigned to the presence of satellite reflections S(-1) and S(+1) [35]. The appearance of better resolved satellites is hindered also by the fact that the bilayer repeat length is fairly large ($\Lambda_{\text{nom}} = 10$ nm) in which case the satellites are already rather close to the main peak [35].

According to Fig. 4a, the XRD patterns of the two nominally identical multilayers prepared from a bath with 0.2 M $\text{Co}(\text{ClO}_4)_2$ concentration do not exhibit any directly visible sign of satellite reflections. These two multilayers are actually also identical in the preparation conditions with the multilayer of our previously reported Co/Cu(Ag) series which was prepared without Ag^+ ion addition (see Fig. 1 of Ref. 12). The latter sample also showed hardly visible satellite reflections only which, however, could be unambiguously identified by a full-profile fitting of the XRD pattern [12].

The weaker or missing satellite reflections for samples prepared with 0.2 M $\text{Co}(\text{ClO}_4)_2$ concentration in the bath, as opposed to the clear satellites for 0.4 M $\text{Co}(\text{ClO}_4)_2$, may come from the fact that at a lower Co^{2+} ion concentration in the bath the amount of Cu incorporated in the magnetic layer is certainly higher due to the fixed value of the magnetic layer deposition current density. The larger Cu content may induce such a large degree of structural disorder that finally leads to a loss of structural coherence along the growth direction and, thus, an important condition for the appearance of satellite reflections is not fulfilled anymore.

Figure 4b shows the XRD patterns of three multilayers with Pb^{2+} ion additions to the bath. For comparison, the XRD pattern with satellite peaks from Fig. 4a (sample prepared with 0.4 M $\text{Co}(\text{ClO}_4)_2$ and 0 % Pb^{2+}) is also added to Fig. 4b. Since the nominal bilayer thickness is the same for all multilayers ($\Lambda_{\text{nom}} = 10$ nm), the shoulder (satellite) positions should also be identical. The two vertical lines in Fig. 4b help visualize that at 0.03 at.% Pb^{2+} ion concentration satellites can be present, but they are probably missing for 0.15 at.% Pb^{2+} ion addition.

It is interesting to note that the addition of a small amount (0.03.%) of Pb^{2+} ions to the bath with 0.2 M $\text{Co}(\text{ClO}_4)_2$ resulted to the appearance of shoulders/satellites reflections with respect to the Pb^{2+} -free solution. This is in accordance with Fig. 3 where one can see that a small amount of Pb^{2+} ions in the bath leads to a reduction of the Cu content with respect to Co in the deposit and, thus, also in the magnetic layer. Therefore, the same explanation applies in Fig. 4b for the presence of satellites in the multilayer prepared from a bath with 0.2 M $\text{Co}(\text{ClO}_4)_2$ and 0.03 % Pb^{2+} as was used for Fig. 4a when comparing the Pb^{2+} -free solutions with low and high $\text{Co}(\text{ClO}_4)_2$ concentrations.

In order to demonstrate more clearly the presence of satellites in our electrodeposited Co/Cu(Pb) multilayers, we have attempted a fitting of the XRD profiles for the three samples for which the shoulders visibly indicated the presence of satellite peaks. Pearson VII type

functions were used to decompose the measured XRD patterns into the main (111) multilayer peak and the S(-1) and S(+1) satellite reflections. The results of decomposition are shown in Fig. 5 for the three samples from Fig. 4b with 0 and 0.03 at.% Pb²⁺ ion concentration (for the other samples measured by XRD, the fitting procedure was not successful). The XRD patterns for the three samples with shoulders could be clearly decomposed and the fitting was characterized by an R² value at least as high as 0.998 in each case. It can be observed that the intensity of the S(-1) satellite is somewhat higher than that of the corresponding S(+1) peak as expected for a Co/Cu multilayer [35].

From the positions of the satellite reflections, the multilayer periodicity Λ_{XRD} can be calculated [36] and we obtained the following bilayer lengths: $\Lambda_{\text{XRD}} = 12.2$ nm (0.4 M Co(ClO₄)₂ and Pb²⁺ = 0 %), $\Lambda_{\text{XRD}} = 13.5$ nm (0.4 M Co(ClO₄)₂ and Pb²⁺ = 0.03 %) and $\Lambda_{\text{XRD}} = 13.0$ nm (0.2 M Co(ClO₄)₂ and Pb²⁺ = 0.03 %). We have calculated the Λ_{XRD} values also from the position of the main (111) peak and the low-angle or high-angle satellite peak positions. The average of the three different Λ_{XRD} values for a given sample was in very good agreement with the value obtained first from the two satellite peak positions. The Λ_{XRD} values are somewhat larger than the nominal bilayer repeat length ($\Lambda_{\text{nom}} = 3$ nm + 7 nm = 10 nm). The very low intensity of the satellites implies a relatively large error for the peak position determination and this may be one major reason for the deviation of the XRD and nominal bilayer lengths. On the other hand, the ratios $\Lambda_{\text{XRD}}/\Lambda_{\text{nom}}$ ranging from 1.22 to 1.35 correspond well to the general trend by considering previous results on electrodeposited Co/Cu multilayers [37,38] and are unrelated to both the anion being present during the deposition and the element added as surfactant (Pb).

Although the indications for the presence or absence of satellites in the XRD patterns of the currently investigated Co/Cu(Pb) multilayers are not completely systematic, we can still draw the following conclusions on the basis of the results presented in Figs. 4 and 5: (i) The presence of satellites around the expected positions corresponding to $\Lambda_{\text{nom}} = 10$ nm is evident at 0 or fairly low Pb²⁺ ion concentrations only. (ii) A high Pb²⁺ ion concentration is unfavorable for the appearance of satellite reflections (shoulders). (iii) The signs for the presence of satellite reflections are weaker if the amount of non-magnetic elements in the magnetic layer is higher.

As to the amount of Pb in the non-magnetic layer, we should refer to Fig. 3 according to which we can estimate that for 0.15 % Pb²⁺ ion concentration, the incorporated amount of Pb

in the Cu layer is about 0.5 at.%. This means that a fairly small amount of Pb in the Cu layer can induce such a degree of disorder during multilayer formation that leads to a reduction of structural coherence as revealed by the disappearance of satellite shoulders. Since it could be seen that the satellites are very weak in all the multilayers produced from a perchlorate bath (both here and in Ref. 12), this deficiency can certainly be assigned to this specific bath. Namely, better defined satellites were observed for electrodeposited Co/Cu multilayers obtained from a sulfate/sulfamate type bath with nominal bilayer repeat lengths up to nearly 13 nm [39].

In any case, with reference to our previous work on electrodeposited Co/Cu(Ag) multilayers [12], the presence of satellites in our electrodeposited Co/Cu(Pb) multilayers can be considered as evidence for the formation of a fairly well-defined layered structure. As we reported in Ref. 12 and will see also in the next section, this degree of layering is sufficient for the observation of a significant multilayer-type GMR effect. Thus, the present work provides further evidence that, whereas the observation of XRD satellites are generally considered as an indicator for the high structural quality of multilayers, the appearance of GMR does not necessarily requires a high degree of structural coherence along the multilayer thickness which feature is otherwise a prerequisite for the formation of satellite reflections.

Magnetoresistance characteristics. — Both the longitudinal and transverse components of the magnetoresistance were studied for Co/Cu(Pb) multilayers electrodeposited from a perchlorate bath with various Pb^{2+} ion concentrations. Four multilayer series were prepared from baths with two different concentrations of $\text{Co}(\text{ClO}_4)_2$: series A, B and C with 0.2 M and series D with 0.4 M. For low Pb^{2+} ion concentrations, the multilayers exhibited a GMR effect (both the LMR and TMR components of the magnetoresistance were negative), whereas for high Pb^{2+} ion concentrations, anisotropic magnetoresistance (AMR) effect ($\text{LMR} > 0$ and $\text{TMR} < 0$) [40,41] was observed. The transition range from GMR to AMR was somewhere between 0.25 % and 0.50% Pb^{2+} ion concentration and varied from series to series. In the following, we will discuss only the results obtained on samples with GMR (series A, B and D; all samples of series C prepared with high Pb^{2+} ion concentrations exhibited AMR behavior).

Figure 6 displays the measured $MR(H)$ curves of Co/Cu(Pb) multilayers prepared from baths with either 0.2 M or 0.4 M $\text{Co}(\text{ClO}_4)_2$ concentration, in each case for zero and 0.15 % Pb^{2+} ion concentrations in the bath.

For both $\text{Co}(\text{ClO}_4)_2$ concentrations, the GMR magnitude was found to decrease with the addition of Pb^{2+} ions to the electrolyte as shown in Fig. 7. There is some scatter of data for samples prepared from the bath with 0.2 M $\text{Co}(\text{ClO}_4)_2$ concentrations (nominally identical series A and B) which results indicate some degree of irreproducibility of the magnitude of the GMR data. We have observed a similar behavior also for Co/Cu(Ag) multilayers [12] and this could be ascribed to an occasional variation of the quality of the substrate used.

If we turn attention again to Fig. 6, we can see a clear difference in the behavior of the field evolution of the magnetoresistance for the two $\text{Co}(\text{ClO}_4)_2$ concentrations. For the case of 0.4 M $\text{Co}(\text{ClO}_4)_2$ concentration, we can observe a practically complete saturation of the $MR(H)$ curves in fairly low magnetic fields (up to about 2 kOe above which only the nearly linear decrease due to the so-called paraprocess [42] prevails). This low saturation field indicates that the observed GMR can be ascribed to spin-dependent scattering events for electrons in a fairly well-defined layered structure consisting of an alternating sequence of ferromagnetic layers and non-magnetic spacer layers [11,43]. On the other hand, for multilayer samples from the bath with 0.2 M $\text{Co}(\text{ClO}_4)_2$ concentration, the saturation occurs in higher magnetic fields only and the non-saturating character gets even stronger with increasing amount Pb. This behavior strongly parallels the results observed also for Co/Cu(Ag) multilayers prepared with the same $\text{Co}(\text{ClO}_4)_2$ concentration [12]. The non-saturating $MR(H)$ curves arise due to the presence of a superparamagnetic (SPM)-type contribution to the GMR [43].

The higher SPM contribution in multilayers prepared from the bath with a lower $\text{Co}(\text{ClO}_4)_2$ concentration (0.2 M) may be attributed to the higher amount of non-magnetic components in the magnetic layer as already discussed above. It was shown in a previous work [44] on electrodeposited Co/Cu multilayers that the increase of the Cu content in the magnetic layer leads to a stronger SPM contribution to the GMR; at the same time, this was also accompanied by a reduction of the XRD satellite intensities as revealed also in the present study (see previous section).

As a comparison with the magnetoresistance results on Co/Cu(Ag) multilayers electrodeposited from a similar perchlorate bath [12], it is noted that whereas for the Co/Cu(Pb) multilayers a GMR to AMR transition is observed for Pb^{2+} ion concentrations between 0.25 % and 0.50 %, the Co/Cu(Ag) multilayers have retained the GMR behavior even up to 15 % Ag^+ ion concentration. For the latter, structural studies indicated a complete

disruption of the layered structure which was in correlation with the dominating superparamagnetic contribution to the GMR in these Co/Cu(Ag) samples [12].

Figure 7 demonstrates that the magnitude of the GMR of the Co/Cu multilayer produced here from the Pb²⁺-free perchlorate bath reproduces our previous result obtained in a study of Co/Cu(Ag) multilayers [12]. For the Co/Cu(Pb) multilayers, the GMR decreases immediately upon the addition of a very small amount of Pb²⁺ ions (as small as 0.01 %) to the bath. This is in contrast to the behavior of electrodeposited Co/Cu(Ag) multilayers [12] where in the range of a few tenths of a percent addition of Ag⁺ ions to the bath induced a sizeable increase of the GMR magnitude.

It might be interesting to compare the differences between Ag and Pb also from another point of view. For the Ag additive, the Ag content in the spacer layer increases monotonously with Ag⁺ ion concentration in the bath and the GMR maximum is in the Ag⁺ ion concentration range (0.1 to 1 %) where the spacer layer has a fairly low Ag content only (at most 1 at.% with respect to Cu) [12]. For the Pb additive, on the other hand, the Pb content exhibits a maximum of about 5 at.% in the Cu layer at around 1.5 % Pb²⁺ ion concentration in the bath (cf. Fig. 3), whereas the GMR decrease sets in already at the smallest Pb²⁺ ion concentration applied. This indicates that the Ag and Pb additives to the spacer layer influence quite differently the layer formation of electrodeposited Co/Cu multilayers, at least from the viewpoint of GMR behavior. This can be related to the different size of the “guest” atoms (Ag or Pb) in the Cu lattice. The relative lattice misfit ($[a_{\text{guest}} - a_{\text{Cu}}]/a_{\text{Cu}}$ where a is the fcc lattice parameter of the pure element) is about 13 % for Ag and about 35 % for Pb. Therefore, it can be easily understood that the structure-destroying impact of Pb appears at a much lower concentration than in the case of Ag. It is also to be noted that Cu is practically immiscible at room temperature with both Ag and Pb; hence, there is no other factor that might lead to the stabilization of either of the metastable mixtures, which further supports the importance of the atomic sizes in the disruption of the native Cu lattice.

Summary

In the present study, the influence of Pb incorporation into electrodeposited Co/Cu multilayer stacks on the structure and GMR was investigated. The aim was to find out if a small amount of Pb in the non-magnetic spacer layer has a similar effect on layer formation

and, thus, on GMR as reported for physically deposited Co/Cu multilayers, where Pb was found to act as an appropriate surfactant element with beneficial effects.

After elaborating an appropriate electrolyte formulation for the electrodeposition of the three metals Co, Cu and Pb from a single bath, multilayers were prepared from a perchlorate electrolyte with different Pb^{2+} ion concentrations in the bath. The incorporation of Pb in the spacer layer of the multilayers exhibited a maximum of 5 at.% Pb with respect to Cu at a Pb^{2+} ion concentration of about 1.5 % in the bath.

A clear GMR effect was observed in multilayers prepared from the perchlorate electrolyte up to a certain Pb^{2+} ion concentration above which an AMR effect was only present. The transition from GMR to AMR happened at a Pb^{2+} ion concentration of 0.2 %. For electrolytes with 0.4 M $\text{Co}(\text{ClO}_4)_2$ concentration and for not too high Pb^{2+} ion concentrations, the observed GMR was mostly dominated by the FM contribution. Such a multilayer-type GMR behavior is due to spin-dependent scattering events of electrons travelling between two ferromagnetic regions with non-aligned magnetizations. This implies that these samples exhibited a fairly well defined layered structure. In the rest of the samples with GMR behavior, the MR(H) curves saturated in higher magnetic fields only which was an indication for the presence of SPM regions in the magnetic layers. The SPM contribution was larger for lower Co^{2+} ion concentrations (promoting high Cu concentrations in the magnetic layers) and for higher Pb^{2+} ion concentrations.

The XRD patterns recorded for a few selected Co/Cu(Pb) multilayers indicated an fcc superlattice structure with a strong (111) texture. In some cases, shoulders on both sides of the (111) reflections appeared at positions corresponding approximately to the satellites of a multilayer with $\Lambda_{\text{nom}} = 10$ nm. A fitting procedure of the measured XRD patterns enabled us to clearly identify the the first order satellite reflections. The satellite intensity reduced both with increasing amount of Pb in the Cu layer and increasing amount of non-magnetic elements incorporated into the magnetic layer. The presence of satellites corresponds to the formation of a layered structure as was also found for electrodeposited Co/Cu(Ag) multilayers from the same perchlorate type bath [12].

In conclusion, it can be established that a perchlorate type bath is appropriate for electrodepositing a multilayered structure in both the Co-Cu-Ag and Co-Cu-Pb system. As far as the structural quality is concerned, the XRD superlattice satellites are very weak even without Ag and Pb addition and the incorporation of these common surfactant elements further reduces the superlattice satellites. Nevertheless, a fairly large room-temperature GMR

of about 8 to 10 % could be observed in these multilayers and the major contribution to this GMR was mainly of the ferromagnetic type, although in some cases a small SPM contribution also appeared. In contrast to the Ag incorporation which in small amount resulted in a slight increase of the GMR [12], according to the present results the Pb addition immediately led to a GMR decrease.

Acknowledgement

This work was supported by the Hungarian Scientific Research Fund (OTKA) through Grants # K 75008 and # K 104696.

References

1. E. Bertel and N. Memmel, *App. Phys. A*, **63**, 523 (1996)
2. J.J. de Miguel and R. Miranda, *J. Phys.: Cond. Matter* **14**, R1063 (2002)
3. J. Camarero, J. Ferrón, V. Cros, L. Gómez, A.L. Vázquez de Parga, J.M. Gallego, J.E. Prieto, J.J. de Miguel and R. Miranda, *Phys. Rev. Lett.* **81**, 850 (1998)
4. J. Camarero, L. Spendeler, G. Schmidt, K. Heinz, J.J. de Miguel and R. Miranda, *Phys. Rev. Lett.* **73**, 2448 (1994)
5. J. Camarero, T. Graf, J.J. de Miguel, R. Miranda, W. Kuch, M. Zharnikov, A. Dittschar, C.M. Schneider and J. Kirschner, *Phys. Rev. Lett.* **76**, 4428 (1996)
6. W. F. Egelhoff, P. J. Chen, C. J. Powell, M. D. Stiles, R. D. McMichael, C. L. Lin, J. M. Sivertsen, J. H. Judy, K. Takano and A. E. Berkowitz, *J. Appl. Phys.* **80**, 5183 (1996)
7. J. Ferron, L. Gomez, J. M. Gallego, J. Camarero, J. E. Prieto, V. Cros, A. De Parga, J. J. De Miguel, R. Miranda, *Surf. Sci.* **459**, 135 (2000)
8. L. Gómez and J. Ferrón, *Phys. Rev. B* **64**, 033409 (2001)
9. M. Marszałek, A. Polit, V. Tokman, Y. Zabala and I. Protsenko, *Surf. Sci.* **601**, 4454 (2007)
10. A. Polit, M. Kac, M. Krupinski, B. Samul, Y. Zabala and M. Marszałek, *Acta Phys. Pol. A* **112**, 1281 (2007)
11. I. Bakonyi and L. Péter, *Progr. Mater. Sci.* **55**, 107 (2010)
12. K. Neuróhr, L. Péter, L. Pogány, D. Rafaja, A. Csik, K. Vad, G. Molnár, I. Bakonyi, *J. Electrochem. Soc.* **162**, D331 (2015)
13. E. Gomez, J. Garcia-Torres, and E. Valles, *Anal. Chim. Acta* **602**, 187 (2007)
14. J. García-Torres, L. Péter, Á. Révész, L. Pogány and I. Bakonyi, *Thin Solid Films* **517**, 6081-6090 (2009)
15. K. Neuróhr, *Electrodeposition and investigation of metallic nanostructures* (Ph.D. Thesis, Eötvös University, Budapest, 2013), in Hungarian
16. M. Alper, W. Schwarzacher, S.J. Lane, *J. Electrochem. Soc.* **144**, 2346 (1997)
17. L. Péter, Z. Kupay, Á. Cziráki, J. Pádár, J. Tóth, I. Bakonyi, *J. Phys. Chem. B* **105**, 10867 (2001)
18. K. Neuróhr, J. Dégi, L. Pogány, I. Bakonyi, D. Ungvári, K. Vad, J. Hakl, Á. Révész, L. Péter, *J. All. Comp.* **545**, 111 (2012)
19. V. Weihnacht, L. Péter, J. Tóth, J. Pádár, Zs. Kerner, C.M. Schneider and I. Bakonyi, *J. Electrochem. Soc.* **150**, C507 (2003)
20. L. Péter, J. Pádár, E. Tóth-Kádár, Á. Cziráki, P. Sóki, L. Pogány and I. Bakonyi, *Electrochim. Acta* **52**, 3813 (2007)
21. A. Bartók, A. Csik, K. Vad, G. Molnár, E. Tóth-Kádár and L. Péter, *J. Electrochem. Soc.* **156**, D253 (2009)
22. L. Péter, Q.X. Liu, Zs. Kerner and I. Bakonyi, *Electrochim. Acta* **49**, 1513 (2004)

23. J.R. Vilche and K. Jüttner, *Electrochim. Acta* **32**, 1567 (1987)
24. J.C. Farmer and R.H. Muller, *J. Electrochem. Soc.* **132**, 39 (1985)
25. R.H. Muller and J.C. Farmer, *Surf. Sci.* **135**, 521 (1983)
26. H. Siegenthaler and K. Jüttner, *J. Electroanal. Chem.* **163**, 327 (1984)
27. L. Péter, Á. Cziráki, L. Pogány, Z. Kupay, I. Bakonyi, M. Uhlemann, M. Herrich, B. Arnold, T. Bauer and K. Wetzig, *J. Electrochem. Soc.* **148**, C168 (2001)
28. E. Pellicer, E. Gómez, E. Vallés, *Surf. Coat. Technol.* **201**, 2351 (2006)
29. E. Gómez, E. Pellicer, E. Vallés, *J. Electroanal. Chem.* **556**, 137(2003)
30. J. Garcia-Torres, E. Gómez, E. Vallés, *J. Appl. Electrochem.* **39**, 233 (2009)
31. M. Pourbaix, *Atlas of Electrochemical Equilibria in Aqueous Solutions*. NACE, Houston, TX, USA, 1974.
32. M. Ujvári, G.G. Láng, G. Horányi, *J. Appl. Electrochem.* **31**, 1171 (2001)
33. G.G. Láng, A. Vrabcz, G. Horányi, *Electrochem. Commun.* **5**, 609 (2003)
34. G.G. Láng, G. Inzelt, A. Vrabcz, G. Horányi, *J. Electroanal. Chem.* **582**, 249 (2005)
35. C. Michaelsen, *Philos. Mag. A* **72**, 813 (1995)
36. E.E. Fullerton, I.K. Schuller, H. Vanderstraeten and Y. Bruynserade, *Physical Review B* **45**, 9292 (1992)
37. N. Rajasekaran, L. Pogány, Á. Révész, B.G. Tóth, S. Mohan, L. Péter and I. Bakonyi, *J. Electrochem. Soc.* **161**, D339 (2014)
38. N. Rajasekaran, J. Mani, B.G. Tóth, G. Molnár, S. Mohan, L. Péter and I. Bakonyi, *J. Electrochem. Soc.* **162**, D204 (2015)
39. D. Rafaja, C. Schimpf, V. Klemm, G. Schreiber and I. Bakonyi, L. Péter, *Acta Mater.* **57**, 3211 (2009)
40. R.M. Bozorth, *Ferromagnetism* (Van Nostrand, New York, 1951)
41. T.R. McGuire and R.I. Potter, *IEEE Trans. Magn.* **11**, 1018 (1975)
42. B. Raquet, M. Viret, J.M. Broto, E. Sondergard, O. Cespedes and R. Mamy, *J. Appl. Phys.* **91**, 8129 (2002); B. Raquet, M. Viret, E. Sondergard, O. Cespedes and R. Mamy, *Phys. Rev. B* **66**, 024433 (2002)
43. I. Bakonyi, L. Péter, Z. Rolik, K. Kiss-Szabó, Z. Kupay, J. Tóth, L.F. Kiss and J. Pádár, *Phys. Rev. B* **70**, 054427 (2004)
44. D. Rafaja, C. Schimpf, T. Schucknecht, V. Klemm, L. Péter, and I. Bakonyi, *Acta Mater.* **59**, 2992 (2011)

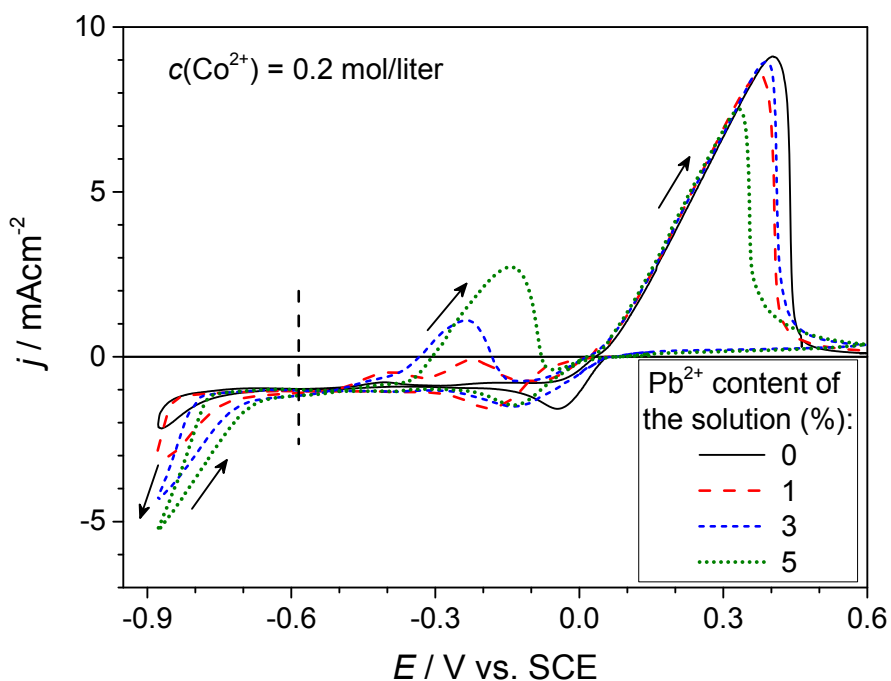


Fig. 1 Cyclic voltammograms of perchlorate electrolytes with 0.2 M $\text{Co}(\text{ClO}_4)_2$ for 0, 1, 3 and 5 % Pb^{2+} ion concentration as indicated. The arrows show the scan direction, while the vertical dashed line indicates the potential applied to deposit the Cu layer.

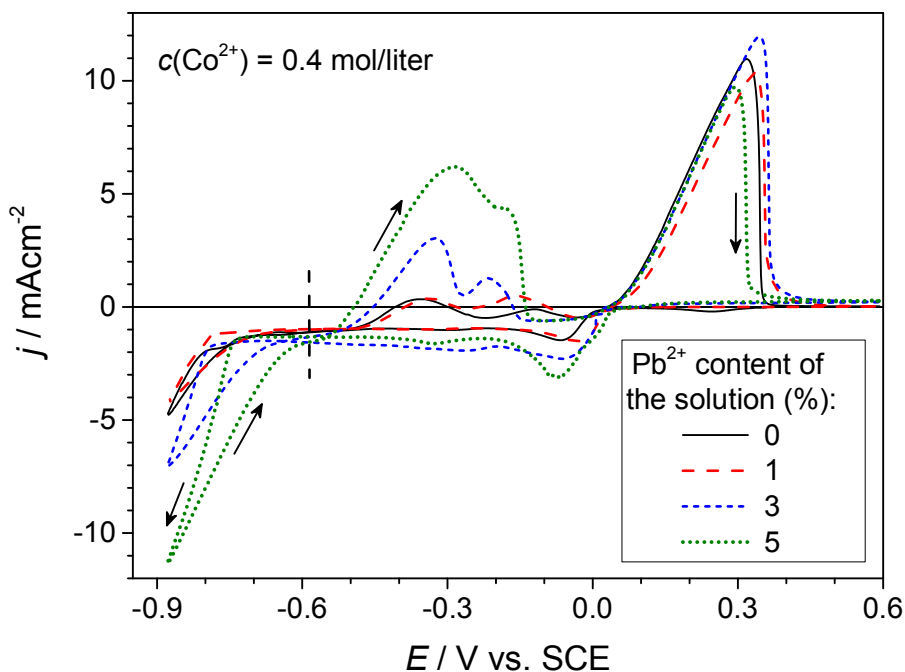


Fig. 2 Cyclic voltammograms of perchlorate electrolytes with 0.4 M $\text{Co}(\text{ClO}_4)_2$ for 0, 1, 3 and 5 % Pb^{2+} ion concentration as indicated. The arrows show the scan direction, while the vertical dashed line indicates the potential applied to deposit the Cu layer.

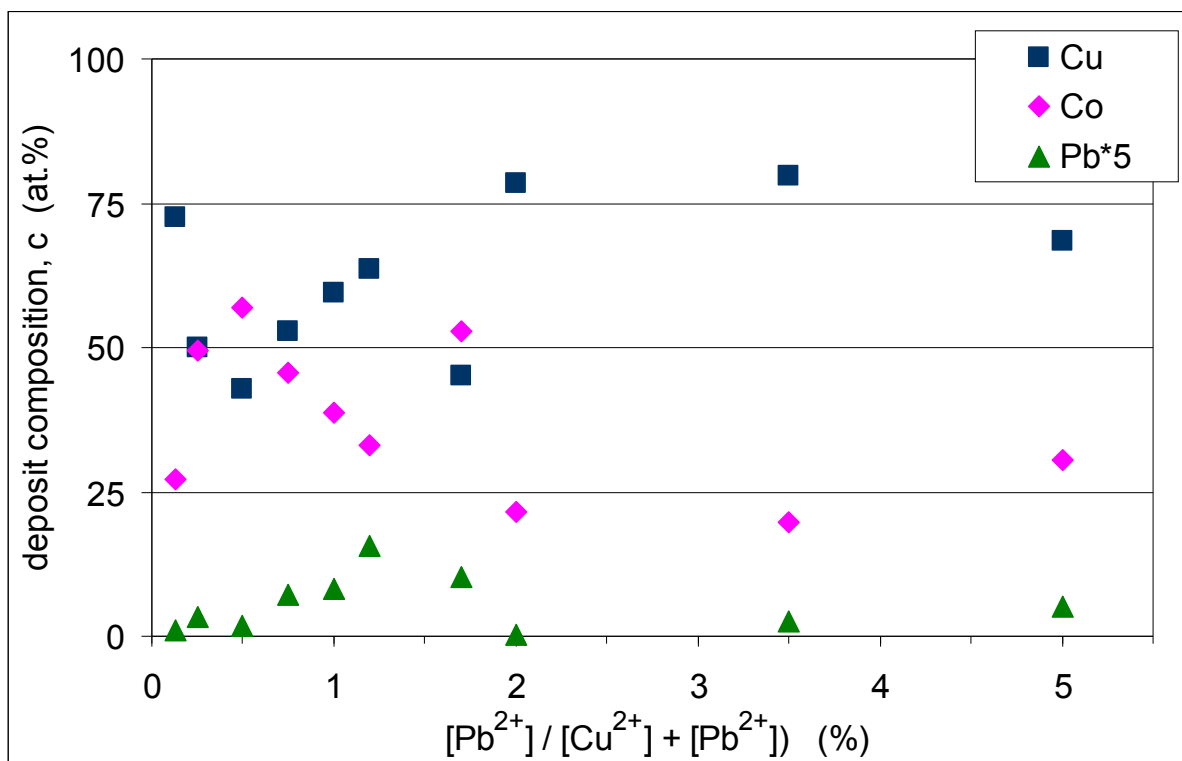


Fig. 3 Composition of Co/Cu(Pb) multilayer deposits obtained from perchlorate baths with 0.2 M $Co(ClO_4)_2$ as a function of the ionic ratio $[Pb^{2+}] / ([Pb^{2+}] + [Cu^{2+}])$ of the ions of the non-magnetic elements in the solution. (Pb molar fraction is multiplied by 5 for the sake of visibility.)

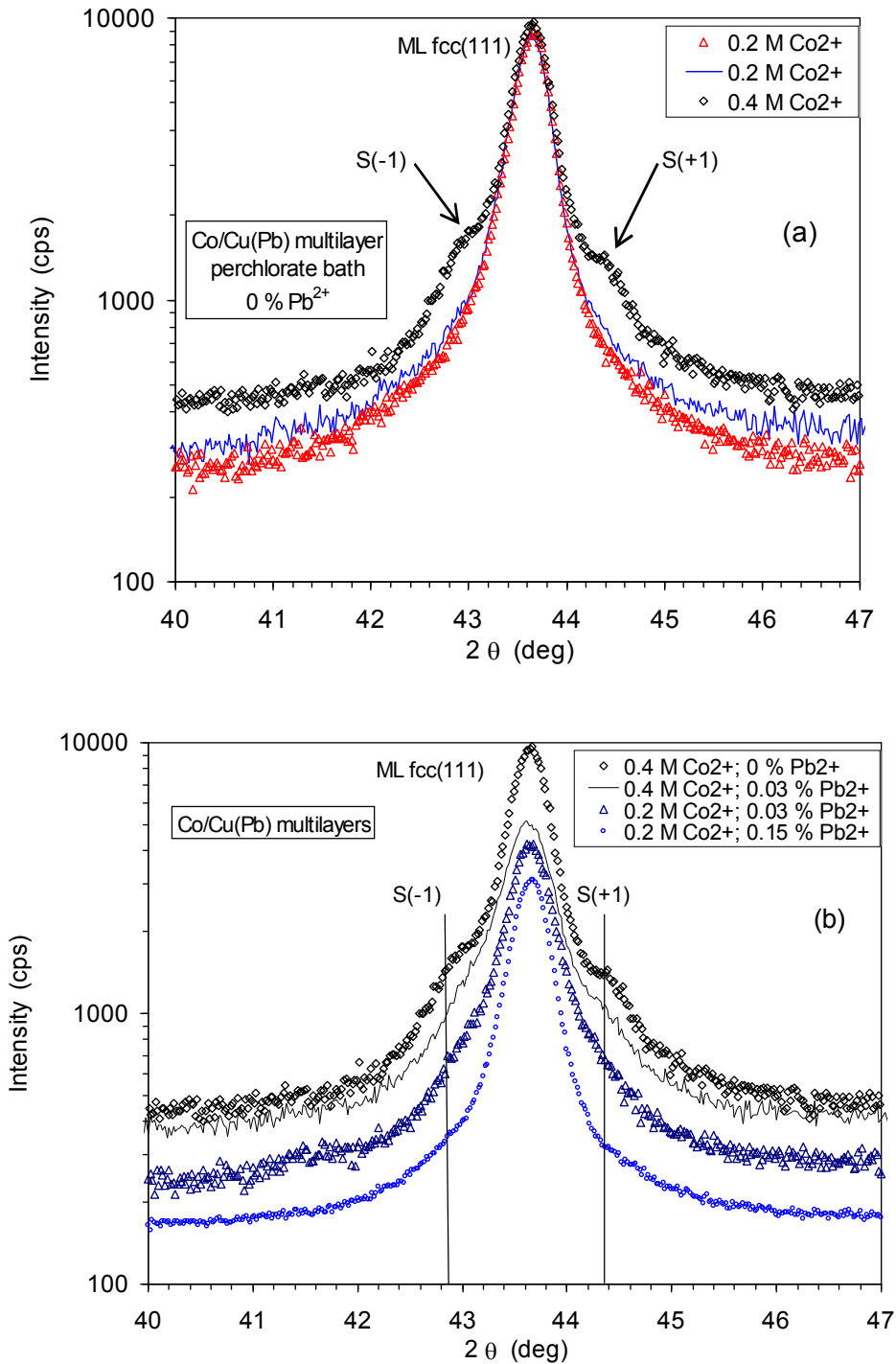
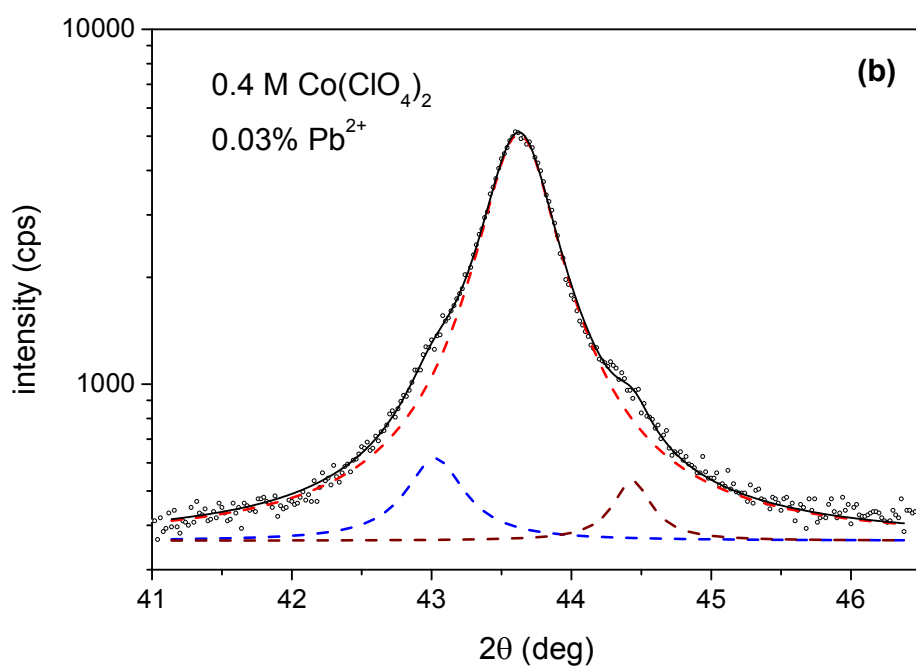
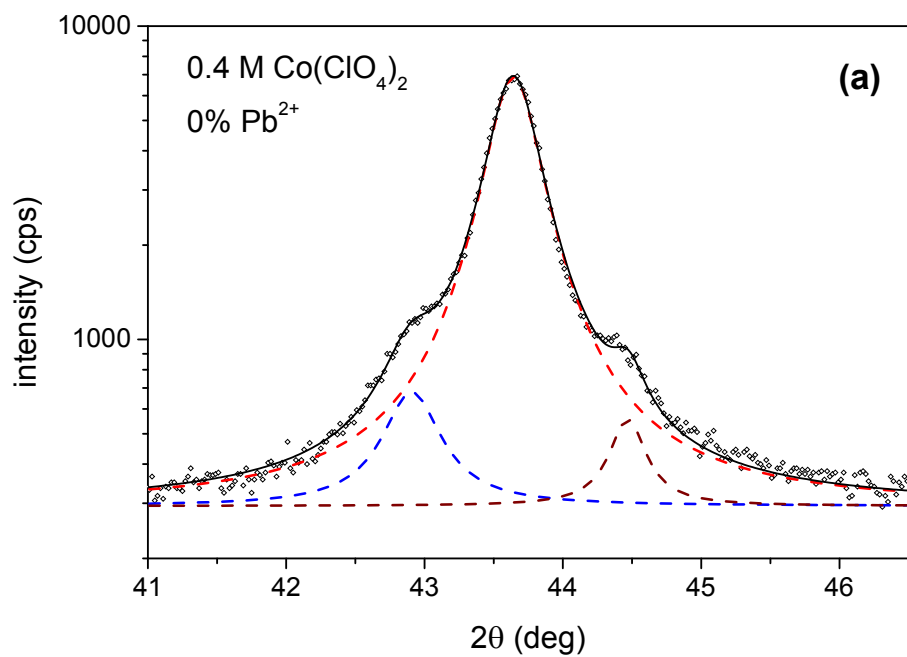


Fig. 4 XRD patterns taken in the vicinity of the (111) multilayer diffraction line for ED Co/Cu(Pb) multilayers prepared from a perchlorate bath with various Pb^{2+} ion and $Co(ClO_4)_2$ concentrations as indicated in the legends. (a) Multilayers prepared without Pb^{2+} addition. The two samples prepared with 0.2 M $Co(ClO_4)_2$ are nominally identical samples obtained in two different series. The arrows point to the shoulders due to the satellite reflections $S(-1)$ and $S(+1)$; (b) Multilayers prepared with various Pb^{2+} ion additions. For reference, the XRD pattern of the multilayer prepared without Pb^{2+} addition and with 0.4 M $Co(ClO_4)_2$ from (a) is also included here. The two vertical solid lines indicate the approximate shoulder positions due to the multilayer satellite reflections $S(-1)$ and $S(+1)$.



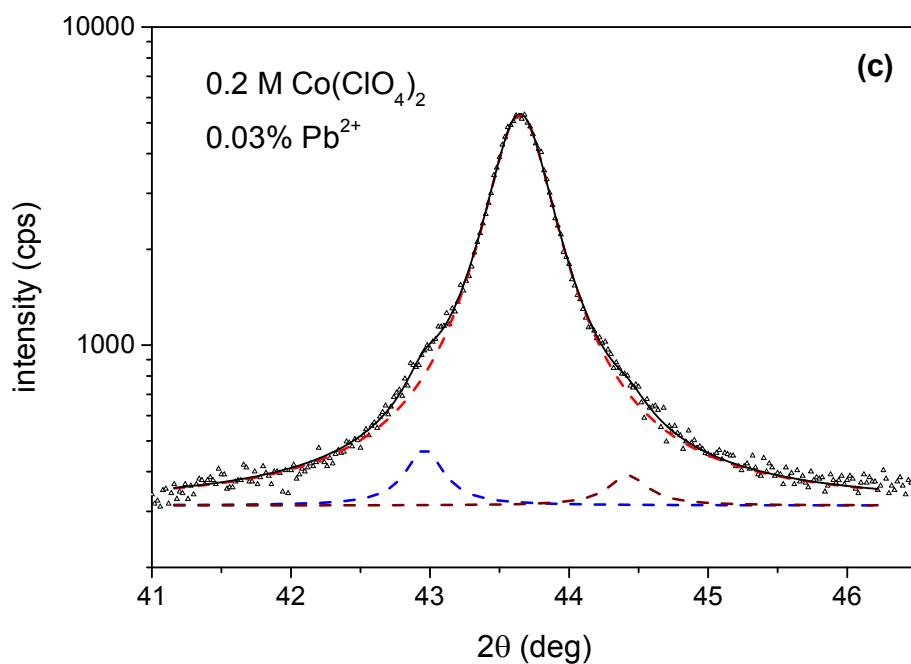


Fig. 5 Decomposition of the measured XRD patterns (data points) to reveal the satellite peaks $S(-1)$ and $S(+1)$ around the main (111) multilayer peak for three electrodeposited Co/Cu(Pb) multilayers shown in Fig. 4: (a) 0.4 M $\text{Co}(\text{ClO}_4)_2$ and 0 Pb^{2+} ion concentration; (b) 0.4 M $\text{Co}(\text{ClO}_4)_2$ and 0.03 % Pb^{2+} ; (c) 0.2 M $\text{Co}(\text{ClO}_4)_2$ and 0.03 % Pb^{2+} ion concentration. Pearson VII type functions (dashed lines) were used to fit the main peak and the two satellites. The sum of the three fitted Pearson VII functions is represented by the solid line. The fit quality (R^2) was at least 0.998 in each case.

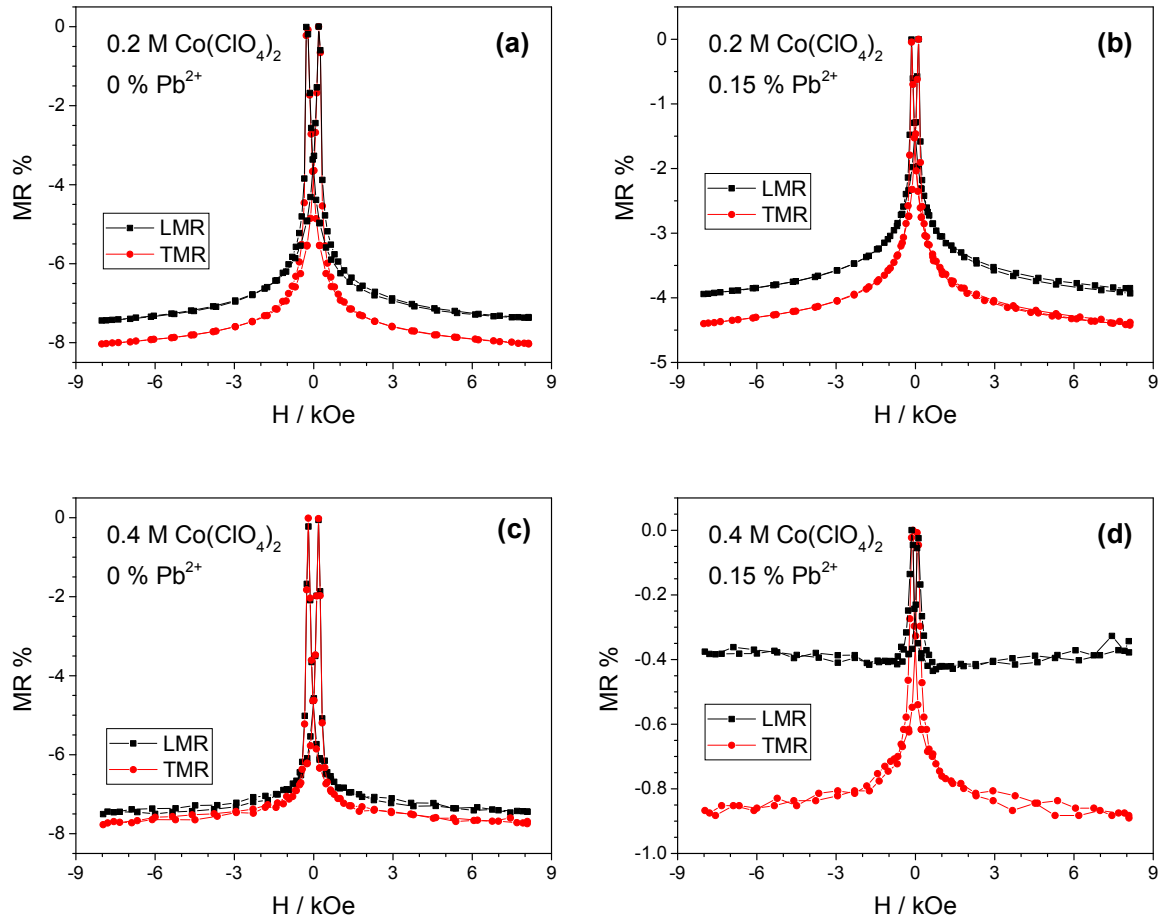


Fig. 6 $MR(H)$ curves measured for four $\text{Co}(3\text{nm})/\text{Cu-Pb}(7\text{nm})$ multilayers prepared from a perchlorate bath containing 0.2 M $\text{Co}(\text{ClO}_4)_2$ (graphs (a) and (b)) or 0.4 M $\text{Co}(\text{ClO}_4)_2$ (graphs (c) and (d)) with various Pb^{2+} ion concentrations as indicated. Squares: LMR component; circles: TMR component.

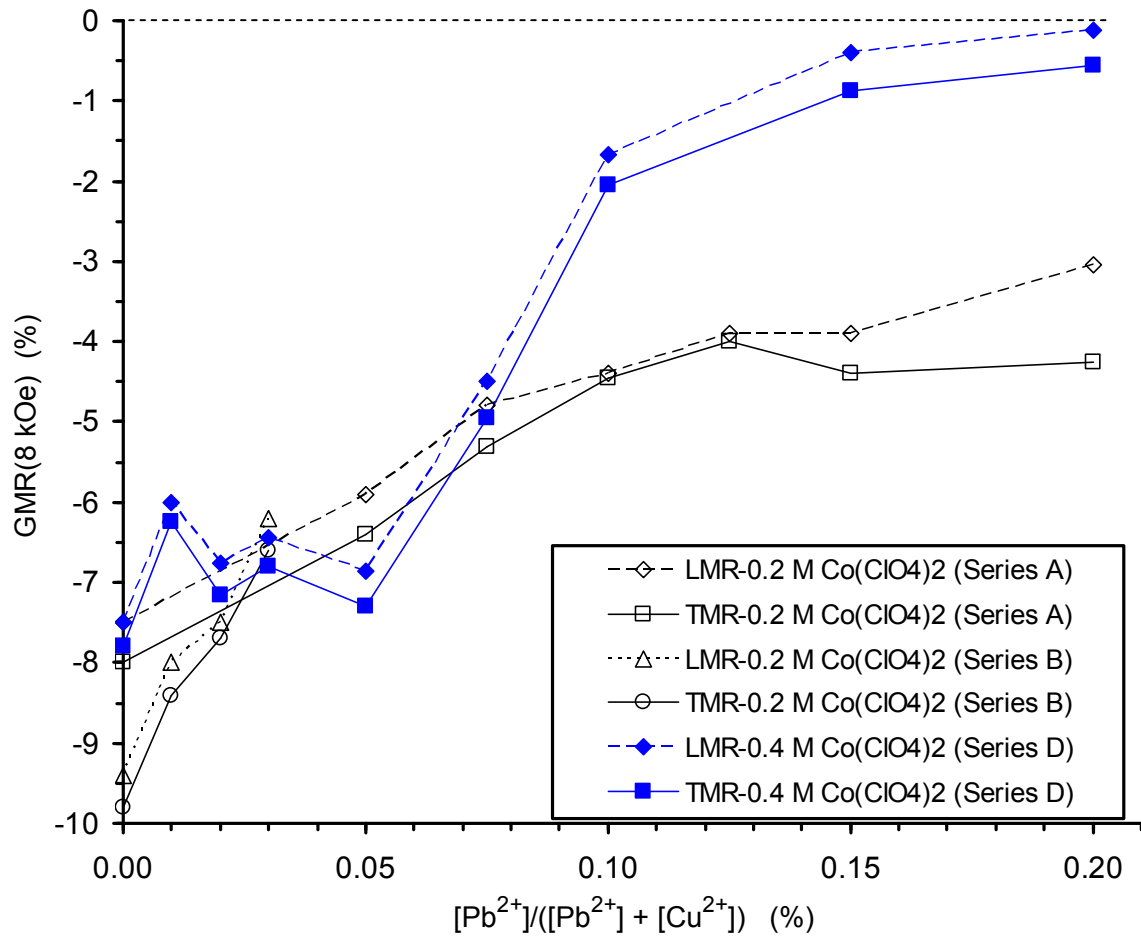


Fig. 7 LMR and TMR values of the GMR measured at $H = 8 \text{ kOe}$ as a function of the Pb^{2+} ion concentration for $\text{Co}(3\text{nm})/\text{Cu-Pb}(7\text{nm})$ multilayers prepared from a perchlorate bath containing 0.2 or 0.4 M $\text{Co}(\text{ClO}_4)_2$.